

## Self-Organized One-Dimensional Electron Systems on a Low-Symmetry Oxide Surface

B. Razaznejad, C. Ruberto, P. Hyldgaard, and B. I. Lundqvist

*Department of Applied Physics, Chalmers University of Technology and Göteborg University, SE-412 96 Göteborg, Sweden*

(Received 21 January 2003; published 13 June 2003)

A new one-dimensional electron gas, metallic over a temperature range of 1–800 K, is predicted on the  $\kappa$ -Al<sub>2</sub>O<sub>3</sub>(00 $\bar{1}$ ) surface by means of density-functional theory (DFT) calculations. The robustness against the Peierls instability is tested using a tight-binding model with DFT-calculated parameters. The critical transition temperature  $T_c$  is shown to be smaller than 1 K. The low value of  $T_c$  makes this system suited for studying Luttinger-liquid (LL) behavior. For future experiments, the LL parameters are estimated, yielding a high electrical conductivity.

DOI: 10.1103/PhysRevLett.90.236803

PACS numbers: 73.20.At, 71.15.Mb

Challenging future nanotechnological applications in, e.g., electronics (ultracompact transistors and circuitry), mechanics (micromachines and sensors), and optics (light-emitting devices) as well as fundamentally interesting electron-electron interaction effects [1], described within Luttinger-Liquid (LL) theory, give strong motivations for studies of the one-dimensional electron gas (1DEG). Today, the broad candidate list for physical manifestation of the 1DEG includes carbon nanotubes (CNT) [2], inorganics (MX chains [3], platinocyanate chains, and charge-density-wave compounds [4,5]), organics [*trans*-polyacetylene (TPA) [6], charge-transfer TTF-TCNQ [7] and Bechgaard salts [8,9]], as well as metallic edge states of nanoclusters [10]. For all of the present single-channel one-dimensional electron systems, however, the structural Peierls metal-insulator (MI) transition of the conductor atoms opens up an energy gap at a relatively high critical temperature  $T_c$ . For inorganics  $T_c$  is  $\sim$ 200 K, for charge-transfer salts  $\sim$ 60 K, and for TPA far above room temperature except upon special difficult doping. This effect confines explorations of the 1D nature of most existing 1DEG realizations to a limited temperature range and complicates their utility.

In this paper, a new 1DEG on the  $\kappa$ -Al<sub>2</sub>O<sub>3</sub>(00 $\bar{1}$ ) surface is predicted using first-principles density-functional theory (DFT) calculations. Figure 1 combines a presentation of structure, electron band structure, and a 3D visualization of the surface-state electron density of  $\kappa$ -Al<sub>2</sub>O<sub>3</sub>(00 $\bar{1}$ ) [11]. The critical temperature of the MI transition is calculated with a tight-binding model, where the parameters are determined with additional DFT calculations [12]. It is shown that  $T_c$  is smaller than 1 K in this 1DEG. Since  $\kappa$ -Al<sub>2</sub>O<sub>3</sub> has a high thermal stability, with a transition temperature  $\sim$ 800 K, this 1D system is metallic over a much wider temperature range than most existing systems mentioned above (Fig. 2). The insulating nature of the surrounding oxide ensures a strong and self-organized electron confinement along the Al chains, to which, for example, scanning-tunneling microscopy tips can establish good electric contacts. Further, as  $\kappa$ -alumina, produced routinely by chemical vapor deposition [13], is a representative of a broader class that we

call structurally flexible ionic crystals with low symmetry [11], 1DEG's are likely to be present on other surfaces of this class [11]. At the same time our prediction offers an alternative, simpler realization than the CNT in that this pure 1DEG is fully decoupled from other (metallic) bands. The low value of  $T_c$  and the simplicity of the band structure make it a good candidate for studying electron-electron correlations, e.g., LL theory, transport through grain boundary [14], and interacting nonlinear transport effects [15]. For this reason, the LL behavior of our system is also characterized.

Our first-principles DFT calculations [11] show that the  $\kappa$ -Al<sub>2</sub>O<sub>3</sub>(00 $\bar{1}$ ) surface is Al terminated, with the Al atoms lying in zigzag lines along the [100] direction. The distance between two adjacent Al lines is  $b = 8.4 \text{ \AA}$ , while the Al-Al distance within the line, projected on [100], is  $a = 2.4 \text{ \AA}$  [Fig. 1(a)]. Because of the charge asymmetry in bulk  $\kappa$ -Al<sub>2</sub>O<sub>3</sub> there exists an excess of electrons at the (00 $\bar{1}$ ) surface compared to an ideal ionic situation [11]. The calculated band structure [Fig. 1(b)] clearly shows a parabolic form along [100] and is almost flat along [010]. From this calculation the Fermi wave vector is estimated to be  $k_F = (\pi/8a)$ . To understand the localization of the surface electrons, the density-of-states profile at the Fermi level is calculated and plotted in real space [Fig. 1(c)]. The surface state is clearly localized around the surface Al atoms, which gives it the character of a pseudo-1D electron gas along [100]. To study the MI transition in this system, which occurs for a Rayleigh mode (a soft surface phonon) with a period of  $(\pi/k_F) = 8a$ , and estimate the critical temperature from first principles, a supercell 4 times larger than the one used here is required. Such a direct calculation is beyond the power of present computer resources. However, the problem can be addressed by bridging the atomic-scale DFT calculations with model studies.

The Su-Schrieffer-Heeger (SSH) Hamiltonian [6], which was originally introduced to study the MI transition in TPA, is adapted to our surface-physics problem. This is achieved by considering the following: (i) The underlying oxide affects the electronic properties of the 1D chain. (ii) The chemical potential  $\mu$  of the chain is

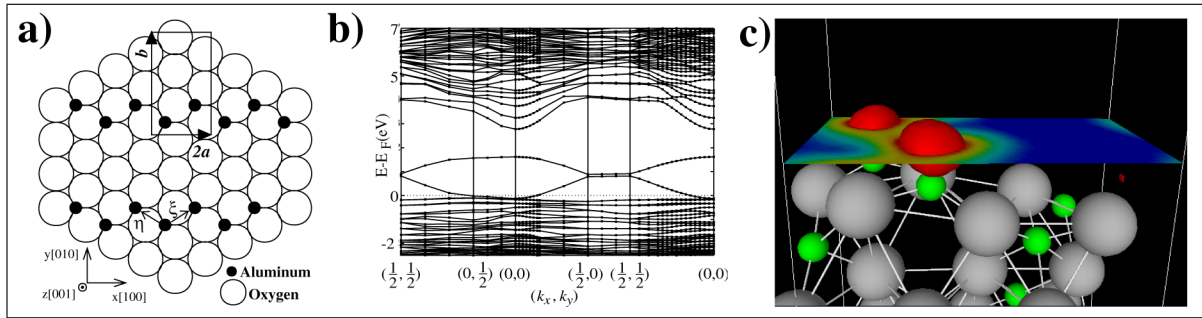


FIG. 1 (color online). (a) Atomic structure of the  $\kappa$ -Al<sub>2</sub>O<sub>3</sub>(00 $\bar{1}$ ) surface. (b) Calculated band structure for the relaxed (00 $\bar{1}$ ) surface of  $\kappa$ -Al<sub>2</sub>O<sub>3</sub>. (c) 3D visualization of the surface-state electron density for the relaxed  $\kappa$ -Al<sub>2</sub>O<sub>3</sub>(00 $\bar{1}$ ) surface at  $E = E_F$ . Large balls are O atoms and small ones are Al atoms.

equal to the underlying bulk oxide but can be calculated by assuming 1D charge conservation due to the large oxide band gap. (iii) The elastic energy is given by that of the soft, longitudinal Rayleigh mode. (iv) Finally, in accordance with the value of  $k_F$ , an eight-band analysis is employed to solve our surface-SSH model. In this model the Hamiltonian can be written as  $H = H_{e,e/ph} + H_{ph}$ , where

$$H_{e,e/ph} = \sum_{n,s} t_{n+1,n} (c_{n+1,s}^\dagger c_{n,s} + c_{n,s}^\dagger c_{n+1,s}) \quad (1)$$

and

$$H_{ph} = \sum_n \left[ \frac{p_n^2}{2M} + \frac{K_{\text{eff}}}{2} (u_{n+1} - u_n)^2 \right]. \quad (2)$$

Here  $u_n$  is the displacement of the  $n$ th Al atom as defined in the longitudinal Rayleigh mode,  $p_n$  its conjugate momentum,  $M$  the mass of the Al atom,  $K_{\text{eff}}$  the effective spring constant, and  $c_{n,s}^\dagger$  ( $c_{n,s}$ ) the fermionic creation (annihilation) operator. The electron-phonon interaction is included in the hopping integral  $t_{n+1,n}$ , which can to first order be expanded around  $\delta = u_{n+1} - u_n = 0$ , giving

$$t_{n+1,n} = t_0 - \alpha(u_{n+1} - u_n), \quad (3)$$

where  $t_0$  is the electronic bandwidth and  $\alpha$  the electron-lattice coupling constant. In the limit of infinite Al mass,

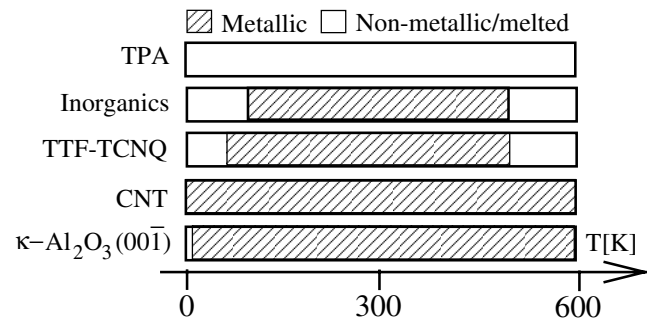


FIG. 2. Comparison of the temperature range for the metallic phases for several 1D systems discussed in the text.

the first term in  $H_{ph}$  can be dropped and for simplicity the spin index is suppressed in the following. Although this model does not take into account explicit electron-electron interactions, some of these are already included when using DFT with the generalized gradient exchange-correlation approximation to determine  $t_0$  and  $\alpha$ .

The Hamiltonian is solved in  $k$  space. The fermionic operators  $c_n$  are Fourier transformed in the reduced zone  $[-k_F, k_F]$  according to  $c_{k\gamma} = [(-i)^\gamma / \sqrt{N}] \times \sum_n e^{-ina(k+2\gamma k_F)} c_n$ , where  $\gamma = 0, \dots, Q-1$ , and  $Q = 8$  in our case, leading to an eight-band analysis. Inverting these relations and using Eq. (3) and the fact that  $u_n = u \cos(2k_F n a)$  under Peierls distortion, the Hamiltonian can be written as  $H = \sum_k \sum_{\alpha,\beta} c_{k\alpha}^\dagger (\Gamma_{k,Q})_{\alpha\beta} c_{k\beta} + H_{ph}(u)$ , where  $H_{ph}(u) = (K_{\text{eff}} N u^2 / 2) [1 - (1/\sqrt{2})]$  and  $(\Gamma_{k,Q})_{\alpha\beta} = \epsilon_{k,\alpha} \Delta_{k,\alpha}$ , and 0, for  $\alpha = \beta$ , for  $\alpha$  and  $\beta$  being nearest neighbors, and for other values of  $\alpha$  and  $\beta$ , respectively.

The  $\epsilon_{k,\gamma}$  are the eigenvalues for  $H_{e,e/ph}$  describing the bands  $\gamma$  without electron-phonon coupling and  $\Delta_{k,\gamma}$  are the coupling terms between two adjacent bands, arising due to the electron-phonon coupling term in the Hamiltonian. Since  $\Gamma$  is symmetric, it is diagonalized by a unitary transformation  $U$ . Putting  $\tilde{c}_{k\gamma} = U c_{k\gamma}$ , the Hamiltonian takes the form  $H = \sum_{k,\gamma} E_{k,\gamma} \tilde{c}_{k\gamma}^\dagger \tilde{c}_{k\gamma} + H_{ph}(u)$ . The  $E_{k,\gamma}$  are now the eigenvalues for  $H_{e,e/ph}$  that describe the bands  $\gamma$  with electron-phonon coupling and  $\tilde{c}_{k\gamma} = \tilde{c}_{k\gamma}^\dagger \tilde{c}_{k\gamma}$  is the number operator for the band  $\gamma$ . The Hamiltonian looks like that for an ideal Fermi gas, with  $\tilde{c}_{k\gamma}^\dagger$  and  $\tilde{c}_{k\gamma}$  being the collective modes of the system.

The critical temperature  $T_c$  is estimated by studying the expression for the total energy, i.e., the phonon energy plus the free energy, per Al atom. This is given by

$$E_T(u) = \frac{H_{ph}(u)}{N} - \frac{2k_B T a}{\pi} \sum_{\alpha=0}^{(Q/2)-1} \int_0^{k_F} \Omega_{k,\alpha}(u, T) dk, \quad (4)$$

where  $k_B$  is the Boltzmann constant,  $\Omega_{k,\alpha}(u, T) = \ln\{1 + \lambda^2 + 2\lambda \cosh[\beta E_{k,\alpha}(u)]\}$ ,  $\lambda = \exp(\beta\mu)$ , and  $\beta = 1/k_B T$ . The chemical potential  $\mu$  of the 1D Al chain must, of course, be equal to the 3D one of the entire

oxide surface but can, effectively, be calculated self-consistently so that the number of electrons in the Al chain is conserved (exactly as in the original SSH model). The underlying surface has a large energy gap between the surface state and the bulk-type conduction band. Using our calculated band structure results [Fig. 1(b)], this energy gap is estimated to be 3.0 eV and the Fermi-distribution function at the conduction band and room temperature is completely vanishing. The number of electrons transferred into and out of the surface state thus remains negligible and surface-state electron conservation applies.

The three model parameters ( $t_0$ ,  $\alpha$ , and  $K_{\text{eff}}$ ) are determined with additional DFT calculations. An accurate determination of  $K_{\text{eff}}$  would require the time-consuming calculation of the full dynamical matrix for all the atoms in the  $\kappa\text{-Al}_2\text{O}_3$  supercell to establish the longitudinal Rayleigh mode. Here, however, a simple model is proposed and analyzed. In this model—the soft phonon model (SPM)—the potential of the system is represented by a pair potential  $\phi$  describing the mutual Al-Al interaction. The effect of the local interactions between the surface and the Al atoms is included in the estimated values of the parameters of the pair potential. In the SPM the Al-chain phonons are softer than in reality, due to the neglect of explicit Al-surface interactions. The SPM will give a lower bound for  $K_{\text{eff}}$  and hence an upper bound for  $T_c$ . In the harmonic approximation such a potential becomes in  $k$  space

$$V(q) = V_0 + \frac{1}{2} \sum_q \sum_{i,j} \sum_{\alpha,\beta} E_{\alpha,\beta}^{ij}(q) Q_{i,q}^\alpha Q_{j,-q}^\beta, \quad (5)$$

where  $E_{\alpha,\beta}^{12}(q) = A[\hat{\xi}_\alpha \hat{\xi}_\beta + \hat{\eta}_\alpha \hat{\eta}_\beta e^{-2iaq}] + B\delta_{\alpha,\beta}[1 + e^{-2iaq}]$ ,  $E_{\alpha,\beta}^{21}(q) = E_{\alpha,\beta}^{12}(-q)$ , and  $E_{\alpha,\beta}^{ii}(q) = -E_{\alpha,\beta}^{12}(0)$ . The  $Q_{i,q}^\alpha$  are the Fourier components of the displacement coordinates in the  $\alpha = \{x, y, z\}$  direction for the Al atom  $i = \{1, 2\}$ ,  $\delta_{\alpha,\beta}$  is the Kronecker delta, and  $\hat{\xi}$  and  $\hat{\eta}$  are the base vectors defined in Fig. 1(a). The parameters  $A = \phi'(d)/d - \phi''(d)$ , and  $B = -\phi'(d)/d$ , where  $d$  is the equilibrium distance between two Al atoms, are fitted to energies calculated with DFT and include the effect of the local interactions between the surface and the Al atoms. Because of the periodic boundary conditions of the supercell, only  $q$  values satisfying  $e^{-2iaq} = 1$  are considered in the fitting.

The lowest acoustic modes from the SPM are investigated. The phonon spectrum  $\omega(q)$  along [100] is shown in Fig. 3. The three acoustic modes in the SPM correspond, in order of increasing energy, to Al motions along the  $z$ ,  $y$ , and  $x$  directions, respectively. Among these the modes in the  $z$  and  $x$  directions model the Rayleigh modes, of which the latter causes the MI transition. The real-space motion for this mode is shown in the inset of Fig. 3. Comparing the energies of this phonon mode at

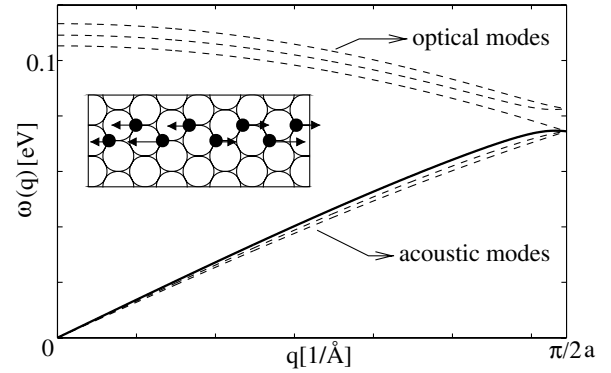


FIG. 3. The surface-Al phonon spectrum for the SPM discussed in the text. The solid line is the acoustic mode along [100] chosen for the MI transition. The inset shows the corresponding real-space motion of the Al atoms.

$2k_F$  with that of a monatomic chain, as given in Eq. (2),  $K_{\text{eff}}$  is estimated to be  $9.0 \text{ eV}/\text{\AA}^2$ .

The parameters  $\alpha$  and  $t_0$  are determined with DFT-calculated band structures for expanded and contracted supercells. Six different values of  $\delta = u_{n+1} - u_n = 0, \pm 0.125, \pm 0.25$ , and  $0.5 \text{ \AA}$  are considered and the obtained  $E(k)$  curves along [100] are fitted to trigonometric functions [ $E = -2t_{n+1,n} \cos(ka)$ ] using the least-square-method approximation. The obtained  $t_{n+1,n}$  values are then inserted into Eq. (3), yielding  $t_0$  and  $\alpha$  (see Table I). The error in the calculated values for  $t_0$  and  $\alpha$  is estimated to be at most 2%.

Using Eq. (4) and the parameters calculated above,  $E_T(u)$  is plotted as a function of the displacement  $u$  at several temperatures (see Fig. 4). The value of  $T_c$  is then determined as the temperature at which the minima of  $E_T(u)$  move from  $u = 0$  to  $u \neq 0$ . Using the estimated parameter values, given in Table I, it is shown that  $T_c$  is

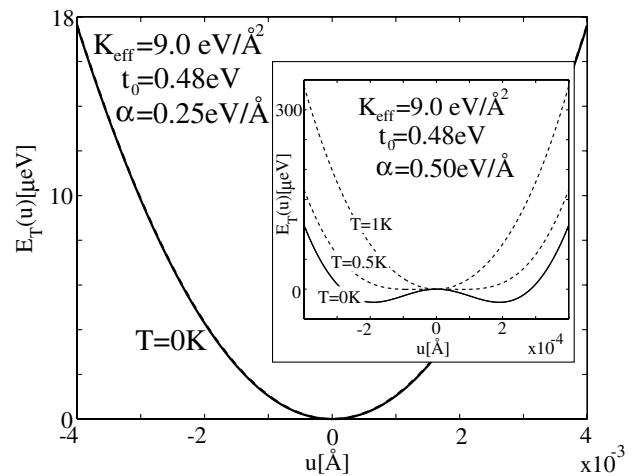


FIG. 4. The total energy per Al atom,  $E_T(u)$ , as a function of the displacement  $u$  at different temperatures  $T$  for estimated parameter values. The inset shows  $E_T(u)$ , when  $\alpha$  is increased to  $0.5 \text{ eV}/\text{\AA}$ , giving the upper bound for  $T_c < 1 \text{ K}$ .

TABLE I. Parameters for our tight-binding model and the estimated  $T_c$  from the SPM discussed in the text.

$K_{\text{eff}}$ (eV/Å <sup>2</sup> )	$t_0$ (eV)	$\alpha$ (eV/Å)	$T_c$ (K)
9.0	0.48	0.25	~0

much smaller than 1 K. Of our calculated model parameters, the calculated  $T_c$  is most sensitive to changes in  $\alpha$  and  $K_{\text{eff}}$ . In particular, a large value for  $\alpha$  and a small one for  $K_{\text{eff}}$  give an upper bound for  $T_c$  and vice versa. The physics behind this is the competition between the electron-phonon interaction energy and the phonon elastic energy, proportional to  $\alpha$  and  $K_{\text{eff}}$ , respectively. Since  $T_c$  is most sensitive to  $\alpha$ ,  $E_T(u)$  is plotted (inset of Fig. 4) keeping all the parameters fixed and using a value of 0.5 eV/Å for  $\alpha$ . This is an extreme value, as the error in  $\alpha$  is less than 2%. Even in this case  $T_c$  remains under 1 K and we conclude that our prediction is robust and that  $T_c$  is smaller than 1 K.

The low value of  $T_c$  makes this system a model system for studying LL physics, which is described by two parameters: the Fermi velocity  $v_F$ , which gives the slope of the linear dispersion, and the renormalized coupling constant  $g$ , which is a measure of the strength of electron-electron interactions. The Fermi velocity  $v_F$  is estimated by  $v_F = 1/\hbar(\partial\epsilon_k/\partial k)|_{k_F}$ . Use of  $\epsilon_k = -2t_0 \cos(ka)$  yields a value of  $0.15 \times 10^8$  cm/s. A rough expression for  $g$  follows by adding a Coulomb energy,  $U = e^2/4\pi\epsilon a$ , where  $\epsilon = \epsilon_0(1 + \epsilon_r)/2$  and  $\epsilon_r = 8.8$  is the dielectric constant of alumina, to the inverse compressibility for a noninteracting 1DEG [14]. This gives  $g \simeq (1 + e^2/8\pi\epsilon a E_F)^{-1/2} = 0.79$ , which implies a 21% reduction of the electrical conductivity  $\sigma$  [16] compared to a non-interacting system. Compared to other systems with LL realization (Table II), our system has a high electrical conductivity.

Two experimentally important aspects for the LL realization of our system are the finite length  $\ell$  of the Al chain and the Coulomb-Coulomb interaction between two chains. The former can be neglected for experimental temperatures above  $T_\ell = \hbar v_F/k_B \ell$  [14]. For  $\kappa\text{-Al}_2\text{O}_3$ ,  $\ell$  is  $\sim 1 \mu\text{m}$  [17], giving  $T_\ell \approx 1$  K. The latter effect is calculated to 0.2 eV, where zero-point fluctuations are taken into account. Although this is a large effect, an individual Al chain can be isolated by “passivation” of the neighboring chains, i.e., by the chemical binding of reactive molecules on top of the Al atoms.

In conclusion, a new and robust 1DEG is predicted on the (00 $\bar{1}$ ) surface of  $\kappa\text{-Al}_2\text{O}_3$  using a combination of DFT and tight-binding model studies. The critical MI temperature is estimated to be smaller than 1 K, implying that the

TABLE II. The Luttinger liquid parameters for three 1D systems.

	$\kappa\text{-Al}_2\text{O}_3(00\bar{1})$	Nanotube [18]	Quantum wire [19]
$v_F$ (cm/s)	$0.15 \times 10^8$	$0.8 \times 10^8$	$0.13 \times 10^8$
$g$	0.79	0.28	0.65

LL should provide a consistent phenomenology for the low-energy properties of this material. As a guideline for experimentalists, the LL parameters are estimated, and their implication on physical properties of our system is discussed. The prospect for *both* key fundamental studies and numerous advanced technical applications is good.

The authors gratefully thank David Langreth for valuable discussions. Support by the Swedish Natural Science Research Council and the Swedish Foundation for Strategic Research (SSF) via Materials Consortia No. 9 and ATOMICS is gratefully acknowledged.

- 
- [1] J. Voit, Rep. Prog. Phys. **58**, 977 (1995).
  - [2] S. Iijima, Nature (London) **354**, 56 (1991).
  - [3] J. T. Gammel *et al.*, Phys. Rev. B **45**, 6408 (1992).
  - [4] C. F. Eagen, S. A. Werner, and R. B. Saillant, Phys. Rev. B **12**, 2036 (1975).
  - [5] M. Sato *et al.*, J. Phys. C **18**, 2603 (1985).
  - [6] W. P. Su, J. R. Schrieffer, and A. J. Heeger, Phys. Rev. Lett. **42**, 1698 (1979).
  - [7] Y. Bouveret and S. Megtert, J. Phys. (Paris) **50**, 1649 (1989).
  - [8] A. Schwartz *et al.*, Synth. Met. **86**, 2129 (1994).
  - [9] V. Vescoli *et al.*, Science **281**, 1181 (1998).
  - [10] M. V. Bollinger *et al.*, Phys. Rev. Lett. **87**, 196803 (2001).
  - [11] C. Ruberto, Y. Yourdshahyan, and B. I. Lundqvist, Phys. Rev. Lett. **88**, 226101 (2002); Phys. Rev. B **67**, 195412 (2003).
  - [12] B. Razaznejad *et al.*, Surf. Sci. (to be published), a preliminary, and oversimplified conference report of the Peierls transition on  $\kappa\text{-Al}_2\text{O}_3$ .
  - [13] S. Vuorinen and J. Skogsmo, Thin Solid Films **193/194**, 536–546 (1990).
  - [14] C. L. Kane and Matthew P. A. Fisher, Phys. Rev. Lett. **68**, 1220 (1992).
  - [15] A. Schiller and S. Hersfield, Phys. Rev. B **51**, 18 (1995).
  - [16] C. L. Kane and Matthew P. A. Fisher, Phys. Rev. Lett. **76**, 3192 (1996).
  - [17] M. Halvarsson, Surf. Coat. Technol. **76–77**, 287–296 (1995).
  - [18] C. L. Kane, L. Balents, and Matthew P. A. Fisher, Phys. Rev. Lett. **79**, 5086 (1997).
  - [19] S. Tarucha, T. Honda, and T. Saku, Solid State Commun. **94**, 413–418 (1995).